Neurobiology of Disease 199 (2024) 106576

Contents lists available at ScienceDirect

Neurobiology of Disease

journal homepage: www.elsevier.com/locate/ynbdi

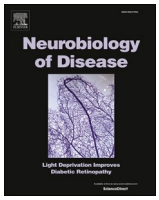

Sunitinib-mediated inhibition of STAT3 in skeletal muscle and spinal cord does not affect the disease in a mouse model of ALS

Massimo Tortarolo [a,1], Andrea David Re Cecconi [a,1], Laura Camporeale [a], Cassandra Margotta [a], Giovanni Nardo [a], Laura Pasetto [a], Valentina Bonetto [a], Mariarita Galbiati [b], Valeria Crippa [b], Angelo Poletti [b], Rosanna Piccirillo [a,2], Caterina Bendotti [a,*,2]

[a] Research Center for ALS, Dept. Neuroscience, Istituto di Ricerche Farmacologiche Mario Negri IRCCS, Via Mario Negri 2, 20156 Milano, Italy
[b] Dipartimento di Scienze Farmacologiche e Biomolecolari "Rodolfo Paoletti", Dipartimento di Eccellenza 2018-2027, Università degli Studi di Milano, via Balzaretti 9, 20133 Milano, Italy

ARTICLE INFO

Keywords:
Amyotrophic lateral sclerosis
STAT3, muscle atrophy
Sunitinib
SOD1
Disease progression
Atrogenes
Spinal cord
Genetic background

ABSTRACT

Variability in disease onset and progression is a hallmark of amyotrophic lateral sclerosis (ALS), both in sporadic and genetic forms. Recently, we found that SOD1-G93A transgenic mice expressing the same amount of mutant SOD1 but with different genetic backgrounds, C57BL/6JOlaHsd and 129S2/SvHsd, show slow and rapid muscle wasting and disease progression, respectively. Here, we investigated the different molecular mechanisms underlying muscle atrophy. Although both strains showed similar denervation-induced degradation of muscle proteins, only the rapidly progressing mice exhibited early and sustained STAT3 activation that preceded atrophy in gastrocnemius muscle. We therefore investigated the therapeutic potential of sunitinib, a tyrosine kinase inhibitor known to inhibit STAT3 and prevent cancer-induced muscle wasting. Although sunitinib treatment reduced STAT3 activation in the gastrocnemius muscle and lumbar spinal cord, it did not preserve spinal motor neurons, improve neuromuscular impairment, muscle atrophy and disease progression in the rapidly progressing SOD1-G93A mice. Thus, the effect of sunitinib is not equally positive in different diseases associated with muscle wasting. Moreover, given the complex role of STAT3 in the peripheral and central compartments of the neuromuscular system, the present study suggests that its broad inhibition may lead to opposing effects, ultimately preventing a potential positive therapeutic action in ALS.

1. Introduction

Amyotrophic lateral sclerosis (ALS) is a severe neurodegenerative disease that gradually affects the neuromuscular system, causing the paralysis of the upper and lower limbs and the muscles responsible for swallowing, breathing and speech. Most ALS patients die of respiratory failure within 3 to 5 years after the onset of symptoms. Approximately 90% of ALS cases are sporadic, while the remaining 10% have inherited genetic causes that are clinically and pathologically indistinguishable from sporadic cases. Despite >50 clinical trials that have been led so far, there is currently no cure for ALS. This lack of success in finding a therapy can be due to the complex nature of the disease, in which

Abbreviations: ALS, amyotrophic lateral sclerosis; CD11c, integrin alpha X chain protein; CD68, Cluster of Differentiation 68; DMD, Duchenne muscular dystrophy; FP, fast progressing; GCM, gastrocnemius muscle; HRP, horseradish peroxidase; IBA1, calcium-binding adapter molecule 1; IBMPFD, Inclusion body myopathy with Paget disease of bone and/or frontotemporal dementia; IFNy, interferon gamma; IL-6, interleukin 6; JAK, Janus kinase; MAFbx, muscle atrophy F box (Atrogin-1); MMP-9, Matrix metalloproteinase-9; MuRF1, muscle RING finger 1; MyoD, Myogenic differentiation factor 1; NFL, Neurofilament light chain; NF-kB, Nuclear Factor kB; NMJ, neuromuscular junction; Nploc4, nuclear protein localization protein 4 homolog; Ntg, non-transgenic; OS, onset stage; PAX7, Paired box protein Pax 7; PNS, peripheral nervous system; PS, pre-symptomatic; SOD1, superoxido dismutase 1; SP, slow progressing; STAT3, Signal Transducers and Activators of Transcription 3; TNFα, tumor necrosis factor alpha; UPS, ubiquitin proteasome system; VEGF, Vascular Endothelial Growth Factor; VEGFR, Vascular Endothelial Growth Factor Receptor.

* Corresponding author.
E-mail address: caterina.bendotti@marionegri.it (C. Bendotti).
[1] Co-first authors.
[2] Co-last authors.

https://doi.org/10.1016/j.nbd.2024.106576
Received 27 March 2024; Received in revised form 14 June 2024; Accepted 21 June 2024
Available online 22 June 2024

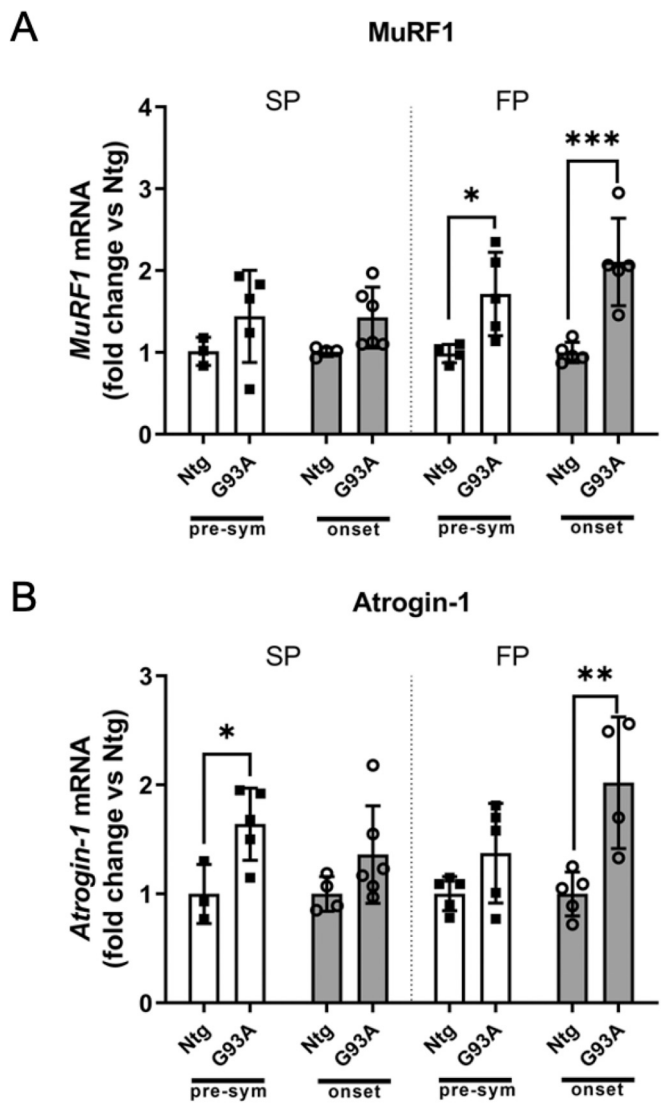

Fig. 1. Increased activation of protein catabolism in GCM muscle reflects faster disease progression in SOD1-G93A mice. *MuRF1* (A) and *atrogin-1* (B) mRNA levels analyzed by real-time quantitative polymerase chain reaction (qPCR) in GCM muscle of SP and FP mice at pre-symptomatic stage and at disease onset, compared with non-transgenic (Ntg) controls. Data are expressed as mean ± SD, $n = 4$–6 mice per group. All data were statistically analyzed using Two-way ANOVA followed by Fisher's LSD post hoc. * $p < 0.05$, ** $p < 0.01$, *** $p < 0.001$.

multiple factors play a role, including oxidative damage, failed protein degradation, intracellular aggregate formation, inflammation, immune system changes and muscle wasting. Another challenge in evaluating the efficacy of treatments is the high heterogeneity in the rate of disease progression, even in cases with a specific genetic cause, such as the SOD1 mutation.

Transgenic mice overexpressing high copies of the G93A mutant of human SOD1 remain the most commonly used animal models for ALS, as they exhibit numerous clinical and histopathologic features that recapitulate both familiar and sporadic forms of the human disease. In these mice, severe and progressive degeneration of spinal motor neurons occurs, leading to motor deficits, marked muscle atrophy and weakness. Typically, mice develop these symptoms at 3–4 months of age and reach complete paralysis of the limbs about 2–3 months later. However, similarly to humans, differences in disease onset, progression rate and survival have been observed in mice with different genetic backgrounds (Heiman-Patterson et al., 2011; Nardo et al., 2016). In particular, we observed significant differences in disease onset and symptom progression between two mouse models of familial ALS, both carrying the same amount of the human SOD1-G93A transgene but on different strains, namely C57BL/6JOlaHsd and 129S2/SvHsd. The transgenic mice on the C57BL/6JOlaHsd genetic background, referred to as "slow progressors" (SP), showed a delayed onset of symptoms and a longer survival of about two and eight weeks, respectively, compared to the SOD1-G93A mice on the 129S2/SvHsd strain, referred to as "fast progressors" (FP). The FP mice exhibited an accumulation of ubiquitinated proteins in the motor neurons, activation of proinflammatory microglia in the spinal cord and dysfunctional peripheral axons earlier than the SP mice (Marino et al., 2015; Nardo et al., 2016).

Conversely, skeletal muscle atrophy and the breakdown of neuromuscular junctions (NMJ) began two weeks earlier in SP mice than in FP mice (Margotta et al., 2023). However, muscle wasting progressed about five times faster in FP mice than in SP mice, leading to complete limb paralysis and end-stage disease about two months earlier (Nardo et al., 2016). While we have shown that activation of myogenesis and an enhanced NMJ response may underlie the compensatory mechanism that reduces the effects of early muscle atrophy in SP mice, it is unclear whether changes in protein homeostasis in the muscles of the two mouse models affect the rate of disease progression. Interestingly, muscle wasting in FP mice was preceded by significant overexpression of interferon-gamma (IFNγ) and CD11c. CD11c is a subunit of the receptor β2-integrin expressed on mouse dendritic cells (DCs) and a subset of mouse monocytes/macrophages, suggesting that an enhanced proinflammatory environment induced by the SOD1 mutant in muscle precedes denervation and atrophy.

There is ample evidence that inflammation is the driving factor for skeletal muscle wasting under various pathological conditions. Inflammatory factors can directly activate several downstream signaling pathways that suppress muscle protein synthesis and over-activate proteolysis, ultimately leading to skeletal muscle atrophy. Signal Transducers and Activators of Transcription 3 (STAT3) and Nuclear Factor-kB (NF-kB) are typical transcription factors that regulate proinflammatory signaling pathways. They both mediate the activation of the ubiquitin-proteasome system (UPS), mainly through the transcription of muscle-specific E3 ubiquitin ligases, including muscle RING finger 1 (MuRF1) and muscle atrophy F-box (Atrogin-1/MAFbx), triggering protein degradation and causing muscle wasting (Guadagnin et al., 2018). These two genes have been named "atrogenes" since their expression is induced in the muscles of rodents undergoing atrophy due to various conditions as fasting, uremia, diabetes and cancer (Lecker et al., 2004). Several studies indicate that the STAT3 signaling pathway is mainly activated by interleukin-6 (IL-6), while NF-kB activation is stimulated by tumor necrosis factor-alpha (TNFα). However, STAT3 has also been shown to be activated by IFNγ to induce muscle wasting independently of IL-6. Therefore, here we asked whether these proteostasis-related signaling pathways may be differently activated in the gastrocnemius muscle of the two SOD1-G93A mouse strains in a way to explain the different rate of muscle atrophy and disease progression of FP mice compared to SP ones.

Catabolic processes associated with inflammation are also responsible for the loss of muscle mass observed in cancer cachexia. Interestingly, we recently found that the p97/VCPATPase complex, another member of the UPS whose gene is mutated in hereditary inclusion body myopathy with Paget disease of bone and/or frontotemporal dementia (IBMPFD) (Kimonis et al., 2008) and ALS (Johnson et al., 2010), is upregulated in atrophying muscles of mouse models of cancer cachexia and ALS, suggesting similar catabolic mechanisms of muscle wasting during fasting and denervation (Piccirillo and Goldberg, 2012; Re Cecconi et al., 2022). Interestingly, inactivation of STAT3 and MuRF1 by the tyrosine kinase inhibitor sunitinib prevented cancer-induced loss of muscle mass (Pretto et al., 2015). Therefore, we investigated whether a similar treatment could also reduce muscle wasting and delay disease progression in ALS mice with rapid disease development.

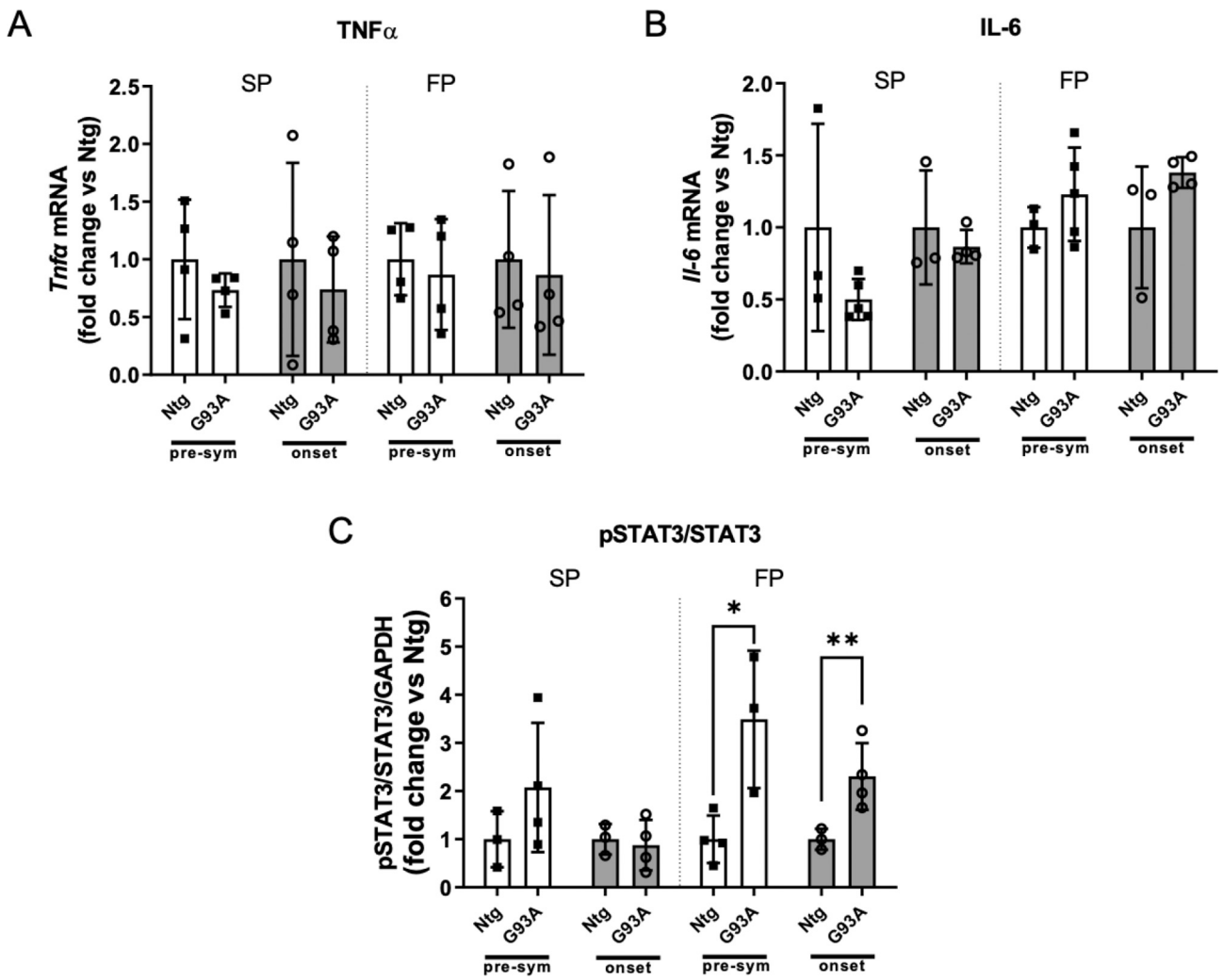

Fig. 2. Increased activation of STAT3 in gastrocnemius occurs only in FP mice. *Tnfα* (A) and *Il*-6 (B) mRNA levels, analyzed by real-time quantitative polymerase chain reaction (qPCR) and pSTAT3 (C) evaluated by Western Blot, in GCM muscle of SP and FP mice at PS stage and disease onset, compared with non-transgenic (Ntg) controls. Data are expressed as mean ± SD, $n = 3$–5 mice per group. All data were statistically analyzed using Two-way ANOVA followed by Fisher's LSD post hoc. * $p < 0.05$, ** $p < 0.01$.

2. Materials and methods

2.1. Mouse models

Female SOD1-G93A transgenic mice on the C57BL/6JOlaHsd or 129S2/SvHsd genetic background, hereafter referred to as SP and FP, respectively, and corresponding non-transgenic (Ntg) female littermates were used (Marino et al., 2015). Gastrocnemius caput medialis (GCM) muscles were harvested from FP and SP mice and corresponding Ntg littermates euthanized at 12 and 14 weeks and 12 and 18 weeks of age, respectively, corresponding to the pre-symptomatic (PS) and onset (OS) stages based on the results of the grip strength test, as previously reported (Margotta et al., 2023). The study was conducted in compliance with standard operating procedures, animal health regulations, and ethical standards of the Istituto di Ricerche Farmacologiche Mario Negri IRCCS (IRFMN) where the studies were carried out. IRFMN adheres to the principles set forth in the following laws, regulations, and guidelines on the care and use of laboratory animals: Italian Law (D.lgs 26/2014; Authorization n.814/2019-PR issued 04 December 2019 by Ministry of Health); Mario Negri Institutional Regulations and Policies providing internal authorization for persons conducting animal experiments (Quality Management System Certificate—UNI EN ISO 9001:2015–Reg. N° 6121); the NIH Guide for the Care and Use of Laboratory Animals (2011 edition) and EU directives and guidelines (EEC Council Directive 2010/63/UE). Mice were maintained at a temperature of 22 ± 2 °C with a relative humidity of 55 ± 10% and 12 h of light/dark cycle. Food (standard pellets) and water were supplied ad libitum.

2.2. Sunitinib treatment schedule and tissue collection

Female SOD1-G93A transgenic mice and corresponding Ntg mice on the 129SvHsd genetic background were used for treatment with sunitinib or placebo.

The mice were randomly divided into four groups. Two groups of SOD1-G93A mice received daily 40 mg/kg/day sunitinib diluted in 0.5% Methocel ($n = 15$) or only 0.5% Methocel (vehicle, n = 15) via oral gavage. Two groups of Ntg mice (n = 15 per group) received the same treatment regimen as controls. Treatment began at 12 weeks of age (before the onset of symptoms). It continued until 14 weeks of age ($n = 6$ per group, symptom onset) or 17 weeks of age ($n = 9$ per group, overt symptomatic stage), when the animals were euthanized. Tissues were collected for biochemical and histologic analyses. Blood was collected in BD microtainer tubes after euthanasia, and serum was collected after 45 min at room temperature (RT) and a 2-min centrifugation at 15000*g* at RT. For histopathological and immunohistochemical analyses, four mice in each group were killed at 17 weeks of age under deep anaesthesia

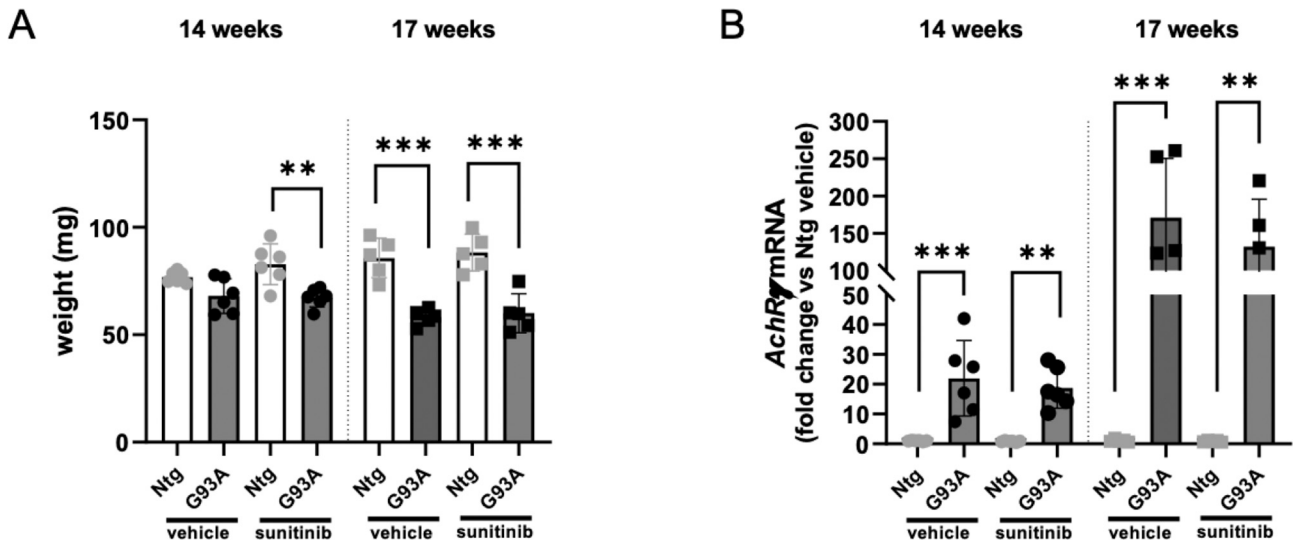

Fig. 3. Sunitinib does not prevent GCM weight loss and denervation in FP mice. Effects of sunitinib treatment on GCM mass (A) and expression of *AchRγ* (B) in FP mice at 14 (onset) and 17 (symptomatic phase) weeks of age, compared with non-transgenic controls (Ntg). The values in panel (A) represents the average weight of the two muscles. Data are expressed as mean ± SD $n = 5$–6 mice per group. All data were statistically analyzed using Two-way ANOVA followed by Fisher's LSD post hoc. ** $p < 0.01$, *** $p < 0.001$.

with a mixture of ketamine (1.75 mg/kg) and medetomidine (1 mg/kg), followed by intracardiac perfusion with 0.1 M PBS and then a solution of 4% paraformaldehyde in 0.1 M PBS. The spinal cords were quickly removed, postfixed in the fixative solution for 24 h, cryopreserved overnight in 30% sucrose solution at 4 °C, frozen in isopentane, cooled in dry ice and stored at −80 °C until analysis.

2.3. Paw grip endurance test

The grip strength test is a non-invasive method to evaluate muscle strength in mice in vivo by exploiting the animals' tendency to grasp a grating with their paws. Mice were placed on a horizontal metal grid, which was then kindly inverted. The performance obtained in the grip strength test was evaluated by a score calculated, according to the following formula:

$$\text{Score} = T_{tot} - \sum_{i=1}^{n} \frac{T_{double\ i}}{2} - \sum_{j=1}^{n} \frac{T_{single\ j}}{4}$$

where *Ttot* is the time animals hang before falling off the grid, *n* is the number of events in which both hind paws (i) or one front or one hind paw (j) were detached from the grid, *Tdouble i* is the number of seconds the (i) event lasted, Tsingle j is the number of seconds the (j) event lasted. The detachment was considered a significant event when it lasted >3 s (Lauranzano et al., 2015). If the mouse was able to cling to the grid for 90 s without significant paw detachment, the maximum score (90) was achieved.

2.4. Immunohistochemistry

Spinal cord immunohistochemistry was performed on free-floating, fixed 30 μm spinal cord coronal sections (one section out of ten from the segment between L2-L5) according to the protocol routinely used in the laboratory (Trolese et al., 2022). The following antibodies and staining were used: goat anti-ChAT antibody (1:200, Merrk-Millipore, Darmstadt, Germany), rabbit anti-IBA1 antibody (1:500, WAKO, Osaka, Japan) and rat anti-CD68 antibody (1:500, Bio-Rad, Milano, Italy) as primary antibodies, while anti-goat Alexa 647 (1:500), anti-rabbit Alexa 647 (1:500) and anti-rat Alexa 488 (1:500) Alexa Fluor® Dyes (Thermo Fisher Scientific, Waltham, Massachusetts, U.S), were used as secondary antibodies. Spinal cord sections were examined using a Nikon NIS Elements confocal microscope. The number of ChAT-immunopositive motor neurons (cell body area > 400 μm^2) was counted for each hemisection (12 sections), and the mean values were used for statistical analysis. Microglia were quantified by determining the area fraction of IBA1 or CD68 immunostaining in the ventral horn using ImageJ software (National Institutes of Health), and the mean values were used for statistical analysis.

2.5. Western blotting

Mice were sacrificed and the spinal cord or GCM muscles were immediately frozen on dry ice and stored at −80 °C. Spinal cord and muscle were homogenized by hand, using a pestle in a 1.5 ml tube, in ice-cold homogenization buffer (RIPA buffer and protease and phosphate inhibitor cocktail from Roche, Basel, Switzerland), centrifuged at 12,000 rpm for 30 min at 4 °C, and the supernatant was collected and stored at −80 °C. Equal amounts of total protein homogenates were loaded onto polyacrylamide gels and blotted onto PVDF membranes (Merk-Millipore) as previously described (Pretto et al., 2015). Membranes were first blocked with 5% dry milk or 5% BSA in TBS with an additional 0.1% Tween (TBS-T) for 1 h (2 h for BSA) at RT and then incubated overnight at 4 °C with one of the following primary antibodies: 1:1000 anti-phosphoTyr705-STAT3 (Cell Signaling, Danvers, Massachusetts, U.S, in 5% BSA), 1:1000 anti-STAT3 (Cell Signaling, in 5% BSA), 1:1000 anti-PAX7 (Merk-Millipore, in 5% dry milk), 1:100 anti-MuRF1 (kindly donated by Prof. Alfred L. Goldberg, Harvard Medical School, Boston, USA, in 5% dry milk), 1:5000 anti-vinculin (Sigma, Burlington, Massachusetts, U.S., in 5% BSA), 1:10000 anti-p97/VCP (Abcam, Cambridge, U.K., in 5% BSA), 1:10000 anti-GAPDH (Sigma, in 5% BSA). Membranes were then washed and incubated with horseradish peroxidase (HRP)-conjugated secondary anti-rabbit antibody (1:2000, Santa Cruz, Dallas, Texas, U.S.) or conjugated to alkaline phosphatase (1:7500, Promega, Madison, Wisconsin, U.S.), and developed using the Luminata Forte Western Chemiluminescent HRP substrate (Merk-Millipore) or with CDP-star substrate (Thermo Fisher Scientific) on the Chemi-Doc XRS system (Bio-Rad Laboratories, Hercules, California, U.S.). Densitometric analysis was performed using ImageLab software (Bio-Rad) or ImageJ software (National Institutes of Health). Ponceau staining or a loading control (vinculin or GAPDH) were used for normalization.

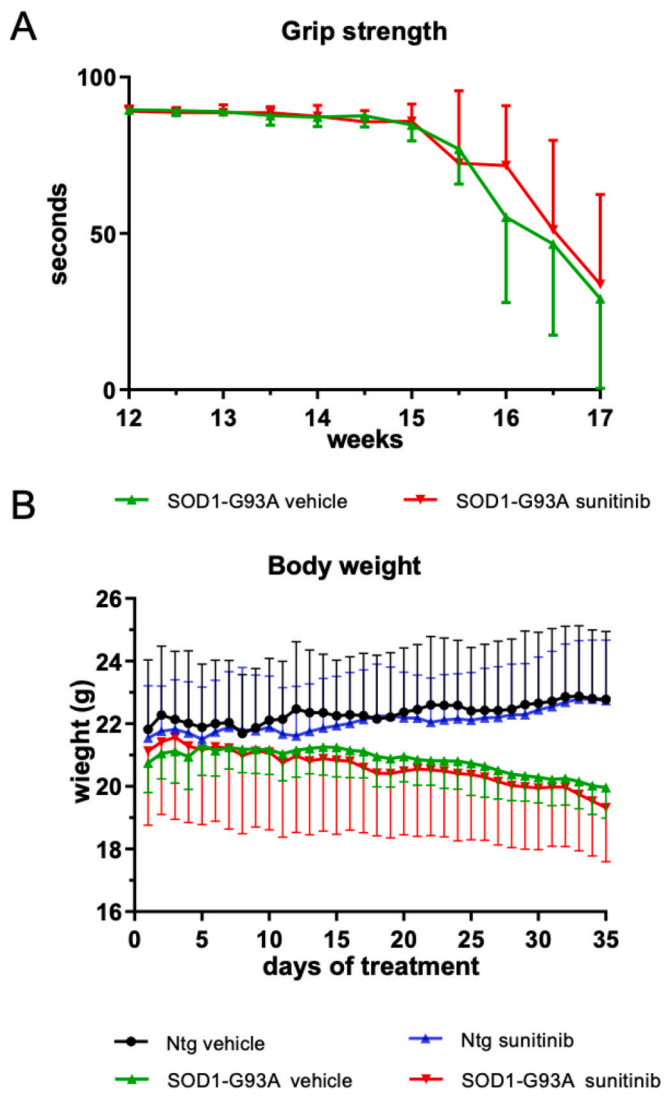

Fig. 4. Sunitinib does not prevent muscle strength deficit nor body weight loss in FP mice. Analysis of paw grip strength (A) and body weight (B) of FP mice treated with sunitinib or vehicle, compared with age- and sex-matched non-transgenic controls (Ntg). Data were expressed as mean ± SD, $n = 9$ mice per group, statistically analyzed using Two-way ANOVA for repeated measures (time) and different groups (treatment) followed by Fisher's LSD post hoc.

2.6. Real-time PCR

Total RNA from the lumbar spinal cord and muscle was extracted in Trizol (Thermo Fisher Scientific), purified (PureLink RNA mini kit, Thermo Fisher Scientific) and quantified using a spectrophotometer (NanoDrop 1000 Spectrophotometer V3.7). RNA samples were treated with DNase I and reverse transcription was performed using the High-Capacity cDNA Reverse Transcription Kit (Thermo Fisher Scientific). The Taq Man (Thermo Fisher Scientific) gene expression assay was performed according to the manufacturer's instructions on duplicate cDNA samples using the 1× Universal PCR Master Mix (BioLine-Meridian Bioscience, Memphis, Tennessee, U.S.) with specific receptor probes: *Tnfα* (Mm00443258_m1, Thermo Fisher Scientific), *Il-6* (Mn00446190_m1, Thermo Fisher Scientific), *Ifnγ* (Mm01168134_m1, Thermo Fisher Scientific), *AchR-γ* (Mm00437419_m1, Thermo Fisher Scientific), *CD68* (Mm03047343_m1, Thermo Fisher Scientific). For analysis of *MuRF1* and *atrogin1* gene expression, frozen gastrocnemius muscles (25 mg) were homogenized using the Tissue Lyser II and stainless-steel glass beads (Qiagen, Hilden, Germany). Total RNA was extracted with TRI-Reagent® (Merck), purified (Direct-zol RNA miniprep Plus Kit, Zymo Research, Irvine. California, U.S.) and quantified using a spectrophotometer (NanoDrop 1000 Spectrophotometer V3.7). Reverse transcription was performed using the High-Capacity cDNA Reverse Transcription Kit (Thermo Fisher Scientific) according to the manufacturer's instructions. Real-time PCR was performed using the CFX 96 Real-Time System (Bio-Rad Laboratories) in a total volume of 10 µl using iTaq SYBR Green Supermix (Bio-Rad Laboratories) on duplicate cDNA samples (10 ng). Primers for the selected genes were designed using the Primer 3 Plus program and purchased from Eurofins Genomics (Ebersberg, Germany). The following primers (final 500 nM) were used: *atrogin-1* (forward: 5'-GAAGAGAGCAGTATGGGGTCA-3′; reverse: 5'-CTTGAGGGGAAAGTGAGACG-3′), *MuRF1* (forward: 5'-ACCTGCTGGTGGAAAACATC-3′; reverse: 5'-AGGAGCAAGTAGGCACCTCA-3′). Melting curve analysis was performed at the end of each PCR assay as a control for specificity. Relative quantification was calculated using the ratio between the number of cycles (Ct) at which the signal exceeded a threshold set within the log phase of each gene and that of the reference *β-actin* gene (Mn02619580_g1, Thermo Fisher Scientific) or ribosomal protein lateral stalk subunit P0 (*Rplp0*). The mean values of triplicate results for each animal were used as individual data for $2^{-\Delta\Delta Ct}$ statistical analysis.

2.7. AlphaLISA assay for matrix metalloproteinase 9 (MMP-9)

The serum level of MMP-9 was measured with an AlphaLISA kit for the murine protein, according to the protocol issued by the manufacturer (#AL519, Revvity, Waltham, Massachusetts, U.S.). AlphaLISA signals were measured using an Ensight Multimode Plate Reader (Revvity).

2.8. Simoa for neurofilament light chain (NFL)

The serum NFL concentration was measured using the Simoa® NF-light™ Advantage (SR-X) Kit (#103400) on the Quanterix SR-X™ platform according to the protocol issued by the manufacturer (Quanterix Corp, Boston, MA, U.S.).

2.9. Statistical analysis

All data are expressed as mean ± SD. The sample size for behavioral tests was based on prior observations in our laboratory regarding the progressive grip strength impairment of ALS mice over eleven time points (repeated measures) and assuming a medium effect size for the treatment. This assumption was made considering that while smaller effect sizes can achieve statistical significance, they often lack clinical or biological relevance. Using G*Power for an F test for repeated measures within-between interaction, we assumed a medium effect size (partial eta squared, $\eta^2p = 0.06$) with a 90% power to detect an effect between two experimental groups, a type I error (α) of 0.05, and a default correlation among repeated measures of 0.50. This calculation indicated a required total sample size of 16 mice, with 8 per experimental condition. This number was then adjusted upwards by approximately 10% to account for attrition (mice dying from causes unrelated to the experiment), leading to the final sample size of 18 mice. Depending on the experiments, one-way or two-way ANOVA was used to compare differences between more than two groups, followed by post hoc Fisher's least significant difference (LSD) with p-value <0.05 as the significance limit. All data sets were tested for the analysis of outliers. GraphPad Prism v.9.01 software (San Diego, CA, U.S.) was used for the statistical analysis.

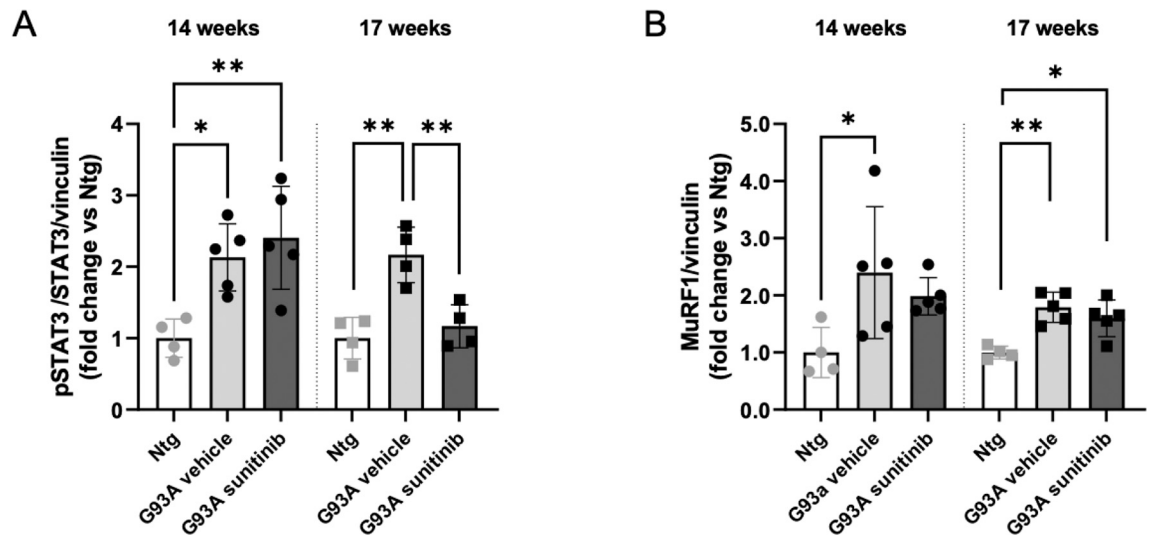

Fig. 5. Sunitinib restrains STAT3 activation, but not MuRF1 induction, in GCM of FP mice. pSTAT3 (A) and MuRF1 (B) protein expression analyzed by Western Blot in GCM of FP mice at 14 (onset) and 17 (symptomatic phase) weeks of age, treated with sunitinib or vehicle and compared with age-matched non-transgenic controls (Ntg). Data are expressed as mean ± SD, $n = 4$–5 mice per group. All data were statistically analyzed using One-way ANOVA followed by Fisher's LSD post hoc, * $p < 0.05$, ** $p < 0.01$.

3. Results

3.1. Enhanced STAT3 activation and protein catabolism in gastrocnemius muscle predict a fast disease progression in SOD1-G93A mice

Skeletal muscle denervation is known to activate the expression of atrogenes, such as MuRF1 and atrogin-1, two muscle-specific E3 ubiquitin ligases that redirect proteins to the proteasome for proteolysis, leading to muscle protein degradation and thus loss of muscle mass. We found that in the GCM muscle of SP mice, mRNA levels of atrogin-1 but not MuRF1 were significantly higher than in Ntg littermates at the PS stage (Fig. 1A, B), when muscles were already partially denervated and atrophied (Margotta et al., 2023). In contrast, they returned to baseline levels at the OS stage, when muscles had already lost 30–40% of their mass (Fig. 1A, B). In FP mice, transcript levels of both MuRF1 and atrogin-1 were also increased at the OS stage, when the muscle was denervated and atrophied (Fig. 1A, B). In contrast, at the PS stage, when there was no denervation or atrophy, only MuRF1 was elevated (Fig. 1A). Thus, protein degradation and the resulting loss of muscle mass in SOD1-G93A mice appears to occur through a rapid increase in atrogenes, which then return to baseline levels in SP mice at the OS stage, while it remains overexpressed in FP mice. A similar pattern was observed for the p97/VCPATPase complex, another key player in the UPS, whose gene is mutated in IBMPFD and ALS and which we have recently shown to play an active role in the degradation of muscle proteins during atrophy induced by cancer or ALS with the help of the Nploc4 adaptor (Re Cecconi et al., 2022). In the SP mice, protein levels of p97 increased significantly only in the PS stage, and returned to baseline levels in the onset and symptomatic stages (Suppl. Fig. 1). In contrast, previously we found that this protein increased in the GCM of FP mice in association with loss of muscle mass and function (Re Cecconi et al., 2022).

These results suggest that upregulation of MuRF1 transcripts precedes denervation-induced muscle atrophy, while transcripts of atrogin-1 and p97/VCP increase when GCM muscle is already impaired by loss of its innervation and mass in FP mice. Since IL-6 and TNFα, as well as the downstream transcription factor STAT3, are potential triggers of the cascade leading to UPS-mediated muscle wasting, we examined the expression levels of these factors in the GCM muscle of both mouse models.

Fig. 2 shows that neither *Tnfα* nor *Il-6* mRNA levels were altered in the GCM of either mouse model at any stage of the disease (Fig. 2A, B). Instead, at the protein level, there was an increase in the pSTAT3/STAT3 ratio in the GCM of FP mice at the PS stage, before muscle denervation and atrophy, and this increase was maintained at the OS stage. In contrast, SP mice show no change in the pSTAT3/STAT3 ratio at any of the stages considered (Fig. 2C, Supplementary Fig. 2). We then investigated whether treatment with sunitinib, a tyrosine kinase inhibitor that we had previously shown to preserve muscle mass in mouse models of cancer-mediated cachexia by inhibiting STAT3 and MuRF1 activation in skeletal muscle (Pretto et al., 2015), could prevent muscle atrophy and delay disease progression in FP mice in which both STAT3 and MuRF1 were activated in muscle.

3.2. Sunitinib treatment did not improve the neuromuscular impairment in FP SOD1-G93A mice

According to the protocol used in our previous study (Pretto et al., 2015), FP mice and their corresponding Ntg littermates were treated daily orally with sunitinib or vehicle. Treatment began at 12 weeks of age, before the onset of motor symptoms and muscle wasting, and continued until 17 weeks of age. We examined the effects of sunitinib treatment on GCM weight at 14 and 17 weeks of age, corresponding to initial and late impairment of skeletal muscle function, respectively. A modest loss of GCM mass was observed as early as 14 weeks of age (12%), which significantly increased to approximately 30% at 17 weeks of age in FP mice treated with vehicle compared to their corresponding Ntg littermates. However, sunitinib treatment had no effect on muscle size at either stage of disease (Fig. 3A). We also investigated the degree of denervation of NMJ by analyzing the overexpression of the *AchRγ* mRNA, the fetal subunit of the cholinergic receptor activated in injured NMJ. The GCM of FP mice exhibited a remarkable 10- and 150-fold increase in *AchRγ* mRNA levels compared to age-matched Ntg mice at 14 and 17 weeks, respectively, indicating pronounced and progressive muscle denervation during disease progression. Sunitinib did not alter the expression of *AchRγ* at all (Fig. 3B).

Accordingly, sunitinib also did not affect the progressive impairment of the paw grip endurance test of FP mice, which reached a deficit of approximately 70% at 17 weeks of age (Fig. 4A). The progressive body weight loss of the FP mice was also not altered by sunitinib (Fig. 4B).

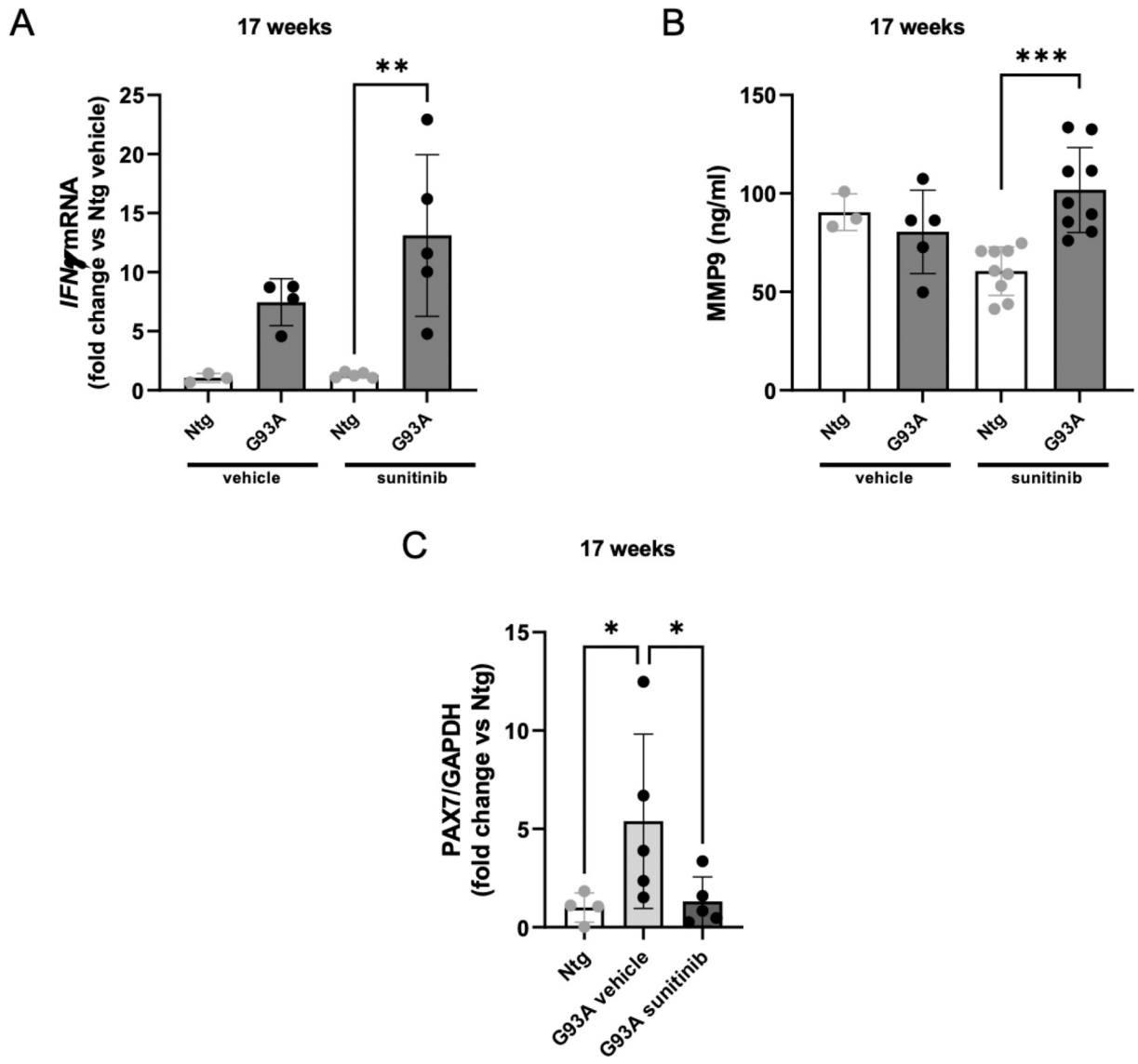

Fig. 6. Sunitinib enhances inflammation and reduces PAX7 induction in the GCM muscle of FP mice. Levels of *IFNγ* mRNA in GCM (A) and MMP9 in serum (B) of FP mice at 17 weeks of age, treated with sunitinib or vehicle and compared with non-transgenic controls (Ntg). (C) PAX7 protein expression in GCM of the same animals. Data are expressed as mean ± SD, $n = 4$–9 mice per group. All data were statistically analyzed using Two-way ANOVA (A, B) or One-way ANOVA (C) followed by Fisher's LSD post hoc. * $p < 0.05$, ** $p < 0.01$, *** $p < 0.001$.

3.3. Sunitinib reduced the activation of STAT3, but not the expression of MuRF1, in the gastrocnemius muscle of FP SOD1-G93A mice

Since the sunitinib treatment protocol was similar to that used to inhibit STAT3 and MuRF1 in mice with cachexia (Pretto et al., 2015), we investigated whether these factors were altered in the GCM of FP mice, despite sunitinib did not affect their muscle mass loss. Using Western blot, we analyzed the phosphorylation of STAT3 and the concentration of MuRF1 in the GCM muscle at the two stages of the disease (at 14 and 17 weeks of age). Sunitinib decreased STAT3 activation in FP mice at 17 but not 14 weeks of age, suggesting that efficient inhibition of the target occurred only after prolonged treatment (Fig. 5A, Supplementary Fig. 3). However, no effect on MuRF1 protein levels was observed in either age group (Fig. 5B, Supplementary Fig. 3).

3.4. Sunitinib enhanced inflammation and hampered the myogenesis in the gastrocnemius muscle of FP SOD1-G93A mice

To determine whether the reduced STAT3 activation induced by sunitinib treatment correlates with reduced inflammation in the GCM of FP mice, we examined the expression of IFNγ, a major inflammatory factor associated with loss of skeletal muscle mass (Shibata et al., 2009). Unexpectedly, we found that sunitinib treatment further increased IFNγ transcript levels in the GCM of SOD1-G93A mice (Fig. 6A), suggesting exacerbated inflammation. Interestingly, levels of MMP-9, an inflammatory marker secreted by neutrophils and macrophages, also tended to be more elevated in the sera of FP mice treated with sunitinib than in mice receiving vehicle (Fig. 6B), although this was not statistically significant. Since chronic high IFNγ levels have anti-myogenic properties, we next examined the levels of PAX7, a hallmark of activated satellite cells, in the GCM of FP mice. Of note, we detected a significant increase in PAX7 in the GCM of vehicle-treated SOD1-G93A mice compared to Ntg littermates, which significantly decreased to the level of Ntg mice after sunitinib treatment (Fig. 6C, Supplementary Fig. 4), suggesting inhibition of myogenesis, which requires further analysis.

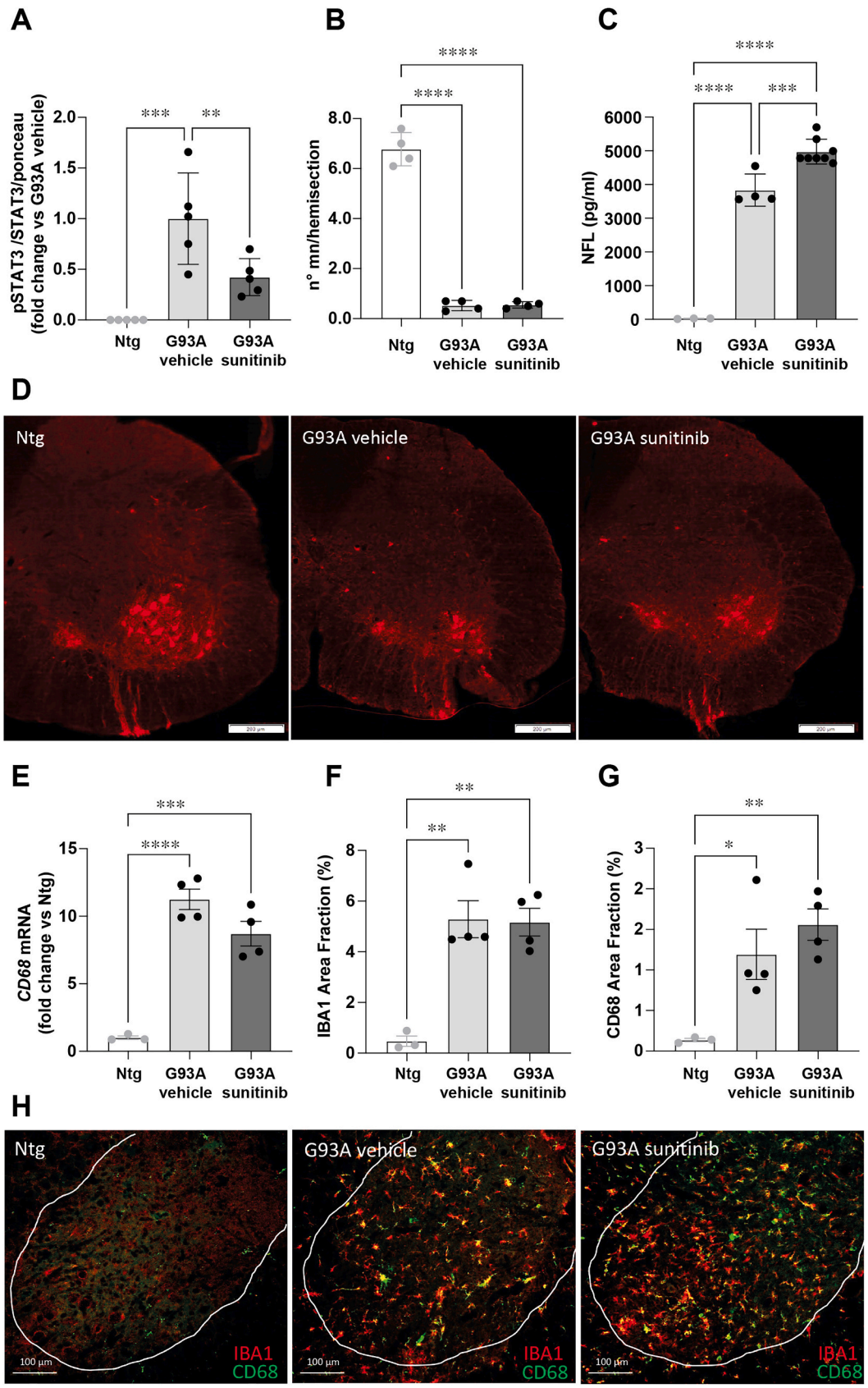

Fig. 7. Sunitinib reduces STAT3 activation in the lumbar spinal cord but does not prevent the motor neuron loss or microglia activation in FP mice. (A) STAT3 activation (pSTAT3) analysis of motor neuron loss by motor neuron count (B, D) and NFL evaluation in serum (C) in lumbar spinal cord of symptomatic, 17-week-old SOD1-G93A mice treated with sunitinib or vehicle and compared with non-transgenic (Ntg) controls. Evaluation of microglia activation by CD68 mRNA levels (E) and IBA1 (F, H) and CD68 (G, H) immunostaining, in lumbar spinal cord of the same animals. Data are expressed as mean ± SD, $n = 4$–8 mice per group. All data were statistically analyzed using One-way ANOVA (B) followed by Fisher's LSD post hoc. * $p < 0.05$, **** $p < 0.0001$.

3.5. Sunitinib reduced STAT3 activation in the lumbar spinal cord but did not prevent motor neuron loss or microglial activation in FP mice

Activation of STAT3 in motor neurons has been proposed as a common pathologic mechanism in both patients and mouse models of ALS (Shibata et al., 2009, 2010). Since sunitinib can cross the blood-brain barrier, we investigated whether long-term treatment with sunitinib could affect pSTAT3 levels in the lumbar spinal cord of FP mice, potentially preventing motor neuron damage and microglial activation. We found that sunitinib reduced the pronounced increase in the pSTAT3/STAT3 ratio in the lumbar spinal cord of symptomatic FP mice (Fig. 7A, Supplementary Fig. 5). However, it did not prevent the significant loss of motor neurons observed in FP mice at this disease stage compared to controls (Fig. 7B, D), nor did it alter microglial activation as evidenced by the increased immunoreactivity of ionized IBA1 and CD68 in the ventral horns of the lumbar spinal cord (Fig. 7F-H). In addition, the increase in CD68 mRNA levels in the spinal cord of sunitinib-treated mice remained unchanged compared to vehicle-treated animals (Fig. 7E). Moreover, serum NFL levels, markers of neuroaxonal damage that were elevated in FP mice compared to age-matched Ntg mice, were even higher after chronic administration of sunitinib, suggesting a deleterious rather than protective effect of this drug on the central nervous system (Fig. 7C).

4. Discussion

Skeletal muscle homeostasis depends on a delicate balance between anabolic and catabolic processes. Various pathological conditions can shift this balance towards the latter, leading to a loss of muscle mass through increased protein breakdown.

We have previously shown that the rate of skeletal muscle atrophy differs between the FP and SP ALS models studied here, although they exhibit the same degree of denervation (Margotta et al., 2023). Specifically, while in FP mice a sudden and rapid muscle atrophy occurs concomitantly with denervation and the beginning of the decrease in muscle strength, in SP mice a similar denervation is accompanied by a moderate and progressive atrophy preceding the onset of symptoms by more than six weeks (Margotta et al., 2023). Interestingly, activation of catabolic markers such as atrogin-1 and p97 was associated with denervation-induced muscle atrophy in both models. However, early and sustained activation of MuRF1 and STAT3 was only found in the muscles of FP mice, even before muscle atrophy and dysfunction occurred. This prompted us to ask whether strategies to inhibit both MuRF1 and the STAT3-based signaling could affect muscle atrophy, particularly in FP mice, and slow their disease progression.

As we have previously shown that sunitinib counteracts cachexia and prevents muscle atrophy in mouse models of renal and colon cancer by inhibiting MuRF1 and the STAT3-pathway (Pretto et al., 2015), we tested the same treatment regimen in the FP ALS model. Indeed, growing evidence from our team and others suggests that there are similarities between cancer- and ALS-induced muscle atrophy, such as the involvement of p97 and Nploc4 in muscle protein degradation (Re Cecconi et al., 2022) and the denervation that occurs in both diseases (Daou et al., 2020; Sartori et al., 2021). Unexpectedly, we found no improvement in muscle atrophy and ALS disease progression in mice treated with sunitinib, despite STAT3 activation was inhibited in both skeletal muscle and spinal cord. However, sunitinib did not alter the expression of MuRF1 in ALS. This is in contrast to the effect observed in mice with cancer-related cachexia (Pretto et al., 2015), suggesting that some of the mechanisms responsible for muscle wasting in cachexia and ALS are different.

The STAT3 signaling plays an essential role in controlling muscle repair and muscle degradation, as it regulates the myogenic capacity of satellite cells after muscle injury and muscle degeneration in muscular dystrophies, cachexia-inducing diseases and other pathologies (Guadagnin et al., 2018). For example, pSTAT3 was detected in satellite cells after four days in culture, and this correlates with the expression of MyoD, suggesting that STAT3 may play a role in the myogenic commitment of these cells (Tierney et al., 2014).

However, the concept that STAT3 activation might promote muscle regeneration does not apply to ALS models. Indeed, we found that the pSTAT3/STAT3 ratio was increased in the GCM of FP mice that did not show activation of Pax7 or overexpression of MyoD at the PS stage. In contrast, this pathway was unchanged in the GCM of SP mice at the PS stage, where we found marked activation of Pax7, sustained activation of MyoD and muscle regeneration (Margotta et al., 2023).

Furthermore, we found that sunitinib treatment prevents the upregulation of Pax7, the hallmark of satellite stem cells, thereby preventing potential myogenesis in the GCM of FP mice. This is in contrast to the observation of Fontelonga and colleagues, who showed that sunitinib, through STAT3 activation promoted myogenesis and muscle regeneration in the mdx mouse model of DMD mice (Fontelonga et al., 2019). Noteworthy, in the Fontelonga study, sunitinib was administered orally three days/week at a dose of 1 mg/kg and four days off, whereas in the present study and in the cachectic mice, the molecule was administered orally at a dose of 40 mg/kg daily for the entire observation period. The stable body weight in our mice receiving the higher dose of sunitinib, compared to controls, suggests the drug did not cause toxicity. Instead, the fact that sunitinib inhibits STAT3 in ALS and cachectic mice, while activates this pathway in mdx model, suggests that the mechanisms underlying the pharmacological action of sunitinib are different between the two protocols and the different diseases.

On the other hand, the pathological mechanisms underlying atrophy in SOD1-G93A and mdx mice seem quite different as demonstrated by the fact that transferring the mdx mutation from the C57 mouse strain to the 129Sv background, there was an improvement in the phenotype associated with more effective muscle regeneration (Calyjur et al., 2016). This is in stark contrast with what we observed in SOD1-G93A models, where 129Sv mice exhibit more severe disease while C57 mice showed slow disease progression associated to immune-mediated muscle fiber regeneration (Margotta et al., 2023; Trolese et al., 2022)

These results illustrate the complexity of the regulatory factors involved in muscle atrophy, which are probably influenced to a large extent by an interplay of various genetic factors and pathological mechanisms. The function of STAT3 signaling has been linked also to its role in modulating the macrophage polarization in both directions, with its activation mainly regulating M2 status (Xia et al., 2023). Interestingly, we reported a remarkable difference in macrophage polarization in skeletal muscle of the two SOD1-G93A mice with a predominant shift towards the M2 phenotype in SP but not in FP mice at PS stage(Margotta et al., 2023), which doesn't line up with the activation of the STAT3 found only in the GCM of FP mice.

Sunitinib treatment successfully reduced STAT3 activation also in the lumbar spinal cord of FP mice, indicating its efficacy in targeting the CNS. However, this reduction did not result in the protection of motor neurons but rather increased serum NFL levels, a biomarker for neuroaxonal degeneration (Benatar et al., 2023). Moreover, the activation of microglia in spinal cord was not prevented by the treatment with sunitinib. Despite reports of persistent activation and nuclear translocation of STAT3 in the spinal cord of ALS patients and the SOD1 mouse models associated with axonopathy and neuroinflammation (Ohgomori et al., 2017), there is no direct evidence that inhibition of STAT3 in motor neurons and glial cells protects motor neurons or improves the disease of SOD1-G93A mice (Shibata et al., 2010). Conversely, studies have shown a correlation between STAT3 activation and motor neuron regeneration after peripheral axotomy (Schwaiger et al., 2000). Indeed, axotomy induces pSTAT3 in the sciatic nerve, which acts as a retrograde signaling transcription factor that promotes axon regeneration in the peripheral nervous system (PNS) (Lee et al., 2004; Qiu et al., 2005). Consequently, inhibition of STAT3 by sunitinib likely impaired the attempt of peripheral axons in ALS mice to regenerate, enhancing the axonal degeneration with subsequent higher NFL serum level. On the other hand, STAT3

activation is crucial for reactive astrocytes to form glial scar following neurodegeneration, which can inhibit neuronal repair and axonal regeneration (Okada et al., 2006). Therefore, by reducing STAT3 activation in spinal cord astrocytes,sunitinib could potentially protect motor neurons and compensate for impaired axonal regrowth. This may explain why sunitinib treatment neither improves nor worsens disease progression and neuropathologic features in SOD1-G93A mice.

5. Conclusion

In summary, while STAT3 is recognized as a common signaling pathway in different forms of muscle wasting associated with distinct diseases, these studies show that the specific mechanisms determining the role of this transcription factor may vary greatly depending on the type of disease-related muscle wasting under investigation. The fact that sunitinib does not affect the phenotype of FP mice does not necessarily mean that STAT3 must be excluded as a potential therapeutic target. Specific inhibitors for STAT3, for example targeting the kinase JAK that activates STAT3 (i.e., jakinibs), have only recently been proposed for ALS (Madaro et al., 2018; Richardson et al., 2023), although none of them have yet been tested in human clinical trials. However, the present study suggests that better and more specific treatment protocols are needed to modulate STAT3 at the peripheral and central levels. A key finding of our study is that early activation of STAT3 and protein catabolism in skeletal muscle can predict rapid disease progression in ALS mice. Although inhibition of STAT3 did not effectively reduce muscle atrophy, its early activation could still serve as a valuable biomarker for muscle atrophy in ALS models. This could have significant implications for both preclinical research and potential clinical applications in humans. Further research is needed to investigate the usefulness of STAT3 as a biomarker and its role in muscle atrophy in different models and human studies.

Funding

This work was supported by Fondazione Italiana di Ricerca per la Sclerosi Laterale Amiotrofica (AriSLA) grant “MUSALS-AChR; Regione Lombardia, Italy, grant “POR FESR 2014–2020 resources Call HUB Ricerca Innovazione-CUP E48I20000000007”; and AFM-Telethon to A. D.R.C., grant n. 24264.

CRediT authorship contribution statement

Massimo Tortarolo: Writing – review & editing, Writing – original draft, Investigation, Formal analysis, Conceptualization. **Andrea David Re Cecconi:** Writing – review & editing, Writing – original draft, Investigation, Funding acquisition. **Laura Camporeale:** Investigation. **Cassandra Margotta:** Investigation. **Giovanni Nardo:** Writing – review & editing, Formal analysis. **Laura Pasetto:** Writing – review & editing, Investigation, Formal analysis. **Valentina Bonetto:** Writing – review & editing. **Mariarita Galbiati:** Writing – review & editing, Investigation, Formal analysis. **Valeria Crippa:** Writing – review & editing, Investigation, Formal analysis. **Angelo Poletti:** Writing – review & editing, Conceptualization. **Rosanna Piccirillo:** Writing – review & editing, Project administration, Funding acquisition, Conceptualization. **Caterina Bendotti:** Writing – review & editing, Writing – original draft, Project administration, Funding acquisition, Conceptualization.

Declaration of competing interest

The authors declare no competing interest.

Data availability

The raw data that supports the findings of this study is available through the Zenodo Repository (https://doi.org/10.5281/zenodo.10848309).

Appendix A. Supplementary data

Supplementary data to this article can be found online at https://doi.org/10.1016/j.nbd.2024.106576.

References

Benatar, M., Wuu, J., Turner, M.R., 2023. Neurofilament light chain in drug development for amyotrophic lateral sclerosis: a critical appraisal. Brain 146 (7), 2711–2716. https://doi.org/10.1093/brain/awac394.

Calyjur, P.C., Almeida, C.F., Ayub-Guerrieri, D., Ribeiro, A.F., Fernandes, S.A., Ishiba, R., Santos, A.L.F.D., Onofre-Oliveira, P., Vainzof, M., 2016. The mdx mutation in the 129/Sv background results in a milder phenotype: transcriptome comparative analysis searching for the protective factors. PLoS One 11 (3), e0150748. https://doi.org/10.1371/journal.pone.0150748.

Daou, N., Hassani, M., Matos, E., De Castro, G.S., Costa, R.G.F., Seelaender, M., Moresi, V., Rocchi, M., Adamo, S., Li, Z., Agbulut, O., Coletti, D., 2020. Displaced Myonuclei in cancer Cachexia suggest altered innervation. Int. J. Mol. Sci. 21 (3), 1092. https://doi.org/10.3390/ijms21031092.

Fontelonga, T.M., Jordan, B., Nunes, A.M., Barraza-Flores, P., Bolden, N., Wuebbles, R. D., Griner, L.M., Hu, X., Ferrer, M., Marugan, J., Southall, N., Burkin, D.J., 2019. Sunitinib promotes myogenic regeneration and mitigates disease progression in the mdx mouse model of Duchenne muscular dystrophy. Hum. Mol. Genet. 28 (13), 2120–2132. https://doi.org/10.1093/hmg/ddz044.

Guadagnin, E., Mázala, D., Chen, Y.-W., 2018. STAT3 in skeletal muscle function and disorders. Int. J. Mol. Sci. 19 (8), 2265. https://doi.org/10.3390/ijms19082265.

Heiman-Patterson, T.D., Sher, R.B., Blankenhorn, E.A., Alexander, G., Deitch, J.S., Kunst, C.B., Maragakis, N., Cox, G., 2011. Effect of genetic background on phenotype variability in transgenic mouse models of amyotrophic lateral sclerosis: a window of opportunity in the search for genetic modifiers. Amyotroph. Lateral Scler. 12 (2), 79–86. https://doi.org/10.3109/17482968.2010.550626.

Johnson, J.O., Mandrioli, J., Benatar, M., Abramzon, Y., Van Deerlin, V.M., Trojanowski, J.Q., Gibbs, J.R., Brunetti, M., Gronka, S., Wuu, J., Ding, J., McCluskey, L., Martinez-Lage, M., Falcone, D., Hernandez, D.G., Arepalli, S., Chong, S., Schymick, J.C., Rothstein, J., Traynor, B.J., 2010. Exome sequencing reveals VCP mutations as a cause of familial ALS. Neuron 68 (5), 857–864. https://doi.org/10.1016/j.neuron.2010.11.036.

Kimonis, V.E., Fulchiero, E., Vesa, J., Watts, G., 2008. VCP disease associated with myopathy, Paget disease of bone and frontotemporal dementia: review of a unique disorder. Biochim. Biophys. Acta 1782 (12), 744–748.

Lauranzano, E., Pozzi, S., Pasetto, L., Stucchi, R., Massignan, T., Paolella, K., Mombrini, M., Nardo, G., Lunetta, C., Corbo, M., Mora, G., Bendotti, C., Bonetto, V., 2015. Peptidylprolyl isomerase A governs TARDBP function and assembly in heterogeneous nuclear ribonucleoprotein complexes. Brain 138 (Pt 4), 974–991. https://doi.org/10.1093/brain/awv005.

Lecker, S.H., Jagoe, R.T., Gilbert, A., Gomes, M., Baracos, V., Bailey, J., Price, S.R., Mitch, W.E., Goldberg, A.L., 2004. Multiple types of skeletal muscle atrophy involve a common program of changes in gene expression. FASEB J. 18 (1), 39–51. https://doi.org/10.1096/fj.03-0610com.

Lee, N., Neitzel, K.L., Devlin, B.K., MacLennan, A.J., 2004. STAT3 phosphorylation in injured axons before sensory and motor neuron nuclei: potential role for STAT3 as a retrograde signaling transcription factor. J. Comp. Neurol. 474 (4), 535–545. https://doi.org/10.1002/cne.20140.

Madaro, L., Passafaro, M., Sala, D., Etxaniz, U., Lugarini, F., Proietti, D., Alfonsi, M.V., Nicoletti, C., Gatto, S., De Bardi, M., Rojas-García, R., Giordani, L., Marinelli, S., Pagliarini, V., Sette, C., Sacco, A., Puri, P.L., 2018. Denervation-activated STAT3-IL-6 signalling in fibro-adipogenic progenitors promotes myofibres atrophy and fibrosis. Nat. Cell Biol. 20 (8), 917–927. https://doi.org/10.1038/s41556-018-0151-y.

Margotta, C., Fabbrizio, P., Ceccanti, M., Cambieri, C., Rufolo, G., D'Agostino, J., Trolese, M.C., Cifelli, P., Alfano, V., Laurini, C., Scaricamazza, S., Ferri, A., Sorarù, G., Palma, E., Inghilleri, M., Bendotti, C., Nardo, G., 2023. Correction: immune-mediated myogenesis and acetylcholine receptor clustering promote a slow disease progression in ALS mouse models. Inflamm. Regener. 43 (1), 25. https://doi.org/10.1186/s41232-023-00276-4.

Marino, M., Papa, S., Crippa, V., Nardo, G., Peviani, M., Cheroni, C., Trolese, M.C., Lauranzano, E., Bonetto, V., Poletti, A., DeBiasi, S., Ferraiuolo, L., Shaw, P.J., Bendotti, C., 2015. Differences in protein quality control correlate with phenotype variability in 2 mouse models of familial amyotrophic lateral sclerosis. Neurobiol. Aging 36 (1), 492–504. https://doi.org/10.1016/j.neurobiolaging.2014.06.026.

Nardo, G., Trolese, M.C., Tortarolo, M., Vallarola, A., Freschi, M., Pasetto, L., Bonetto, V., Bendotti, C., 2016. New insights on the mechanisms of disease course variability in ALS from mutant SOD1 mouse models. Brain Pathol. (Zurich, Switzerland) 26 (2), 237–247. https://doi.org/10.1111/bpa.12351.

Ohgomori, T., Yamasaki, R., Takeuchi, H., Kadomatsu, K., Kira, J.-I., Jinno, S., 2017. Differential activation of neuronal and glial STAT3 in the spinal cord of the SOD1G93A mouse model of amyotrophic lateral sclerosis. Eur. J. Neurosci. 46 (4), 2001–2014. https://doi.org/10.1111/ejn.13650.

Okada, S., Nakamura, M., Katoh, H., Miyao, T., Shimazaki, T., Ishii, K., Yamane, J., Yoshimura, A., Iwamoto, Y., Toyama, Y., Okano, H., 2006. Conditional ablation of

Stat3 or Socs3 discloses a dual role for reactive astrocytes after spinal cord injury. Nat. Med. 12 (7), 829–834. https://doi.org/10.1038/nm1425.
Piccirillo, R., Goldberg, A.L., 2012. The p97/VCP ATPase is critical in muscle atrophy and the accelerated degradation of muscle proteins. EMBO J. 31 (15), 3334–3350. https://doi.org/10.1038/emboj.2012.178.
Pretto, F., Ghilardi, C., Moschetta, M., Bassi, A., Rovida, A., Scarlato, V., Talamini, L., Fiordaliso, F., Bisighini, C., Damia, G., Bani, M.R., Piccirillo, R., Giavazzi, R., 2015. Sunitinib prevents cachexia and prolongs survival of mice bearing renal cancer by restraining STAT3 and MuRF-1 activation in muscle. Oncotarget 6 (5), 3043–3054. https://doi.org/10.18632/oncotarget.2812.
Qiu, J., Cafferty, W.B.J., McMahon, S.B., Thompson, S.W.N., 2005. Conditioning injury-induced spinal axon regeneration requires signal transducer and activator of transcription 3 activation. J. Neurosci. 25 (7), 1645–1653. https://doi.org/10.1523/JNEUROSCI.3269-04.2005.
Re Cecconi, A.D., Barone, M., Gaspari, S., Tortarolo, M., Bendotti, C., Porcu, L., Terribile, G., Piccirillo, R., 2022. The p97-Nploc4 ATPase complex plays a role in muscle atrophy during cancer and amyotrophic lateral sclerosis. J. Cachexia. Sarcopenia Muscle 13 (4), 2225–2241. https://doi.org/10.1002/jcsm.13011.
Richardson, P.J., Smith, D.P., de Giorgio, A., Snetkov, X., Almond-Thynne, J., Cronin, S., Mead, R.J., McDermott, C.J., Shaw, P.J., 2023. Janus kinase inhibitors are potential therapeutics for amyotrophic lateral sclerosis. Transl. Neurodegener. 12 (1), 47. https://doi.org/10.1186/s40035-023-00380-y.
Sartori, R., Hagg, A., Zampieri, S., Armani, A., Winbanks, C.E., Viana, L.R., Haidar, M., Watt, K.I., Qian, H., Pezzini, C., Zanganeh, P., Turner, B.J., Larsson, A., Zanchettin, G., Pierobon, E.S., Moletta, L., Valmasoni, M., Ponzoni, A., Attar, S., Sandri, M., 2021. Perturbed BMP signaling and denervation promote muscle wasting in cancer cachexia. Sci. Transl. Med. 13 (605), eaay9592. https://doi.org/10.1126/scitranslmed.aay9592.
Schwaiger, F.W., Hager, G., Schmitt, A.B., Horvat, A., Hager, G., Streif, R., Spitzer, C., Gamal, S., Breuer, S., Brook, G.A., Nacimiento, W., Kreutzberg, G.W., 2000. Peripheral but not central axotomy induces changes in Janus kinases (JAK) and signal transducers and activators of transcription (STAT). Eur. J. Neurosci. 12 (4), 1165–1176. https://doi.org/10.1046/j.1460-9568.2000.00005.x.
Shibata, N., Kakita, A., Takahashi, H., Ihara, Y., Nobukuni, K., Fujimura, H., Sakoda, S., Sasaki, S., Iwata, M., Morikawa, S., Hirano, A., Kobayashi, M., 2009. Activation of signal transducer and activator of transcription-3 in the spinal cord of sporadic amyotrophic lateral sclerosis patients. Neurodegener. Dis. 6 (3), 118–126. https://doi.org/10.1159/000213762.
Shibata, N., Yamamoto, T., Hiroi, A., Omi, Y., Kato, Y., Kobayashi, M., 2010. Activation of STAT3 and inhibitory effects of pioglitazone on STAT3 activity in a mouse model of SOD1-mutated amyotrophic lateral sclerosis. *Neuropathology: official journal of the Japanese society of*. Neuropathology 30 (4), 353–360. https://doi.org/10.1111/j.1440-1789.2009.01078.x.
Tierney, M.T., Aydogdu, T., Sala, D., Malecova, B., Gatto, S., Puri, P.L., Latella, L., Sacco, A., 2014. STAT3 signaling controls satellite cell expansion and skeletal muscle repair. Nat. Med. 20 (10), 1182–1186. https://doi.org/10.1038/nm.3656.
Trolese, M.C., Scarpa, C., Melfi, V., Fabbrizio, P., Sironi, F., Rossi, M., Bendotti, C., Nardo, G., 2022. Boosting the peripheral immune response in the skeletal muscles improved motor function in ALS transgenic mice. Mol. Ther. 30 (8), 2760–2784. https://doi.org/10.1016/j.ymthe.2022.04.018.
Xia, T., Zhang, M., Lei, W., Yang, R., Fu, S., Fan, Z., Yang, Y., Zhang, T., 2023. Advances in the role of STAT3 in macrophage polarization. Front. Immunol. 14, 1160719. https://doi.org/10.3389/fimmu.2023.1160719.